

Photodegradation of Molecular Iodine on SiO2 Particles: Influence of Temperature and Relative Humidity

A. Figueiredo, Rafal Strekowski, L. Bosland, A. Durand, H. Wortham

▶ **To cite this version:**

A. Figueiredo, Rafal Strekowski, L. Bosland, A. Durand, H. Wortham. Photodegradation of Molecular Iodine on SiO2 Particles: Influence of Temperature and Relative Humidity. Journal of Nuclear Engineering and Radiation Science, 2021, 7 (3), 10.1115/1.4048846 . hal-03214498

HAL Id: hal-03214498
https://hal.science/hal-03214498

Submitted on 1 May 2021

HAL is a multi-disciplinary open access archive for the deposit and dissemination of scientific research documents, whether they are published or not. The documents may come from teaching and research institutions in France or abroad, or from public or private research centers.

L'archive ouverte pluridisciplinaire **HAL**, est destinée au dépôt et à la diffusion de documents scientifiques de niveau recherche, publiés ou non, émanant des établissements d'enseignement et de recherche français ou étrangers, des laboratoires publics ou privés.



Distributed under a Creative Commons Attribution 4.0 International License

Photodegradation of molecular iodine on SiO_2 particles: Influence of temperature and relative humidity

A. Figueiredo [a,b], R.S. Strekowski *[,a], L. Bosland [b], A. Durand [a], H. Wortham [a]

[a] Aix Marseille Univ, CNRS, LCE, Marseille, France
[b] Institut de Radioprotection et de Sûreté Nucléaire, PSN-RES/SAG/LETR, Cadarache, France

Abstract

A molecular derivatization method followed by gas chromatographic separation coupled with mass spectrometric detection was used to study photo-degradation of molecular I_2 adsorbed on solid SiO_2 particles. The heterogeneous photo-degradation of I_2 was studied as a function of temperature and relative humidity in synthetic air to better understand its environmental fate. Two sets of experiments were carried out. In the first set of experiments, the temperature was T = (298±1)K and relative humidity was varied from ≤ 2% to 75% RH under given experimental conditions. In the second set of experiments, the relative humidity within the Pyrex bulb was 40%RH and the temperature was varied from 283±1 ≤ T(K) ≤ 323±1. The obtained results show a considerably enhanced atmospheric lifetime of molecular iodine adsorbed on solid media that does not depend on relative humidity of the environment. The obtained results show that the rate constant for the photolysis of molecular iodine adsorbed on model SiO_2 particles depends on temperature and is reported to be $J\ (\mathrm{T}) = (1.24 \pm 1.4) \times 10^{-2} \times \exp[(1482 \pm 345)/\mathrm{T}]/\mathrm{s}$ over the measured temperature range. The heterogeneous atmospheric residence time (τ) of I_2 adsorbed on solid media is calculated to range from 2 to 4.1 hours. The experimentally obtained heterogeneous lifetime of I_2 is shown to be considerably longer than its destruction by its principal atmospheric sink, photolysis. The observed enhanced atmospheric lifetime of I_2 on heterogeneous media will likely have direct consequences on the atmospheric transport of I_2 that influences the toxicity or the oxidative capacity of the atmosphere.

Introduction

Atmospheric aerosols are known to play important direct and indirect roles in climate regulation [1]. Aerosols' direct climate regulation properties are attributed to their light-scattering characteristics and aerosols' indirect effects include their ability to act as cloud condensation nuclei (CCN), thus, affecting the Earth's energy budget. In turn, aerosols' optical and CCN properties are governed by their chemical composition and reactivity. Molecular iodine and other iodine containing organic compounds are known to make up an important fraction of the marine and coastal sites aerosol content [2]. Ocean emissions account for the majority of molecular iodine emissions into the natural atmosphere [3,4] with the measured I_2 mixing ratios ranging from few pptv to 300±100 pptv [5–13]. More recently, molecular iodine emissions have gained an increased level of interest in the scientific community and executive branches of some governments following the major nuclear power plant accident in Fukushima (Japan) [14,15] where significant radioactive molecular iodine and other organic iodides emissions were observed (among other radioisotope emissions) in the atmosphere when the reactor containment structure was damaged.

While the atmospheric reactivity of gas phase I_2 is now well understood and characterized [12,16], our understanding of the heterogeneous reactivity on atmospheric aerosols remains feeble at best. This is problematic because aerosols belong to an intricate and tangled atmospheric system where the aerosol number concentrations range from few thousands to several hundreds of thousands of particles per cubic centimeter (1/cm) [17,18]. This represents a Brobdingnagian number of potential surfaces for gas-phase I_2–particle heterogeneous reactivity, a hypothesis that has been supported by early laboratory experiments [19–22] that show that gas phase I_2 readily adsorbs on solid atmospheric particles. Further, we showed in a recent study that the photodegradation rate of molecular iodine on solid media was very different (much lower) from the photodegradation rate in the homogeneous phase [23]. This

difference in reactivity will likely have a direct impact on the long-range gas-phase I_2 atmospheric transport and reactive fate [24,25]. That is, different environmental factors may influence the atmospheric behavior and fate of molecular iodine adsorbed on solid particles. For example, particles exposed to RH values ranging from 30% to 100% at ambient temperature may result in surface mono- or multi-layer water films [26]. These surface water layers may induce important changes in the heterogeneous reactivity since the kinetics of many surface reactions depend strongly on the type of particle phase, surface morphology and surface physico-chemical properties [27]. Further, in the case of an accidental radioiodine release from a nuclear powerplant facility, its dispersion and atmospheric behavior will need to be reassessed to ensure the radioprotection of the population and application of the appropriate mitigation strategies.

In this work we focus on the kinetics of the photodegradation of molecular iodine adsorbed on model solid media as function temperature and humidity. Only stable iodine-127 isotope is studied and the reactivity of the radioisotope iodine-131 is not considered. This allowed us to carry out all the laboratory experiments without any significant radiological safety concerns. Further, since iodine-127 and iodine-131 have the same number of valence electrons, their reactivity is expected to be equivalent. However, the heterogeneous photo-reactivity of the molecular iodine adsorbed on solid media may be affected by the difference in the molar masses of iodine-127 and iodine-131. It is not believed that the kinetic isotope effect (KIE) resulting from the mass-dependence of collision frequencies plays a major role in the heterogeneous interactions of molecular iodine [28,29]. While the KIE has been shown to play a role in the homogeneous reactions of OH radicals with non-methane hydrocarbons containing C-12 and C-13 isotopes [30,31], this effect has been shown to be relatively low (1‰ to ~16‰) for carbon isotopes [30,32]. Also, the KIE is expected to decrease with increasing molecular mass [30].

Consequently, it is assumed that the KIE due to the small difference between the molecular mass of iodine-127 and iodine-131 is negligible [28,29].

The apparatus and the experimental protocol used to study the photo-degradation of molecular iodine on solid media has been documented before [23]. Therefore, only details relevant to this work are given below.

Experimental

A schematic representation of the experimental system used in this work is published elsewhere [23]. A 500 cm^3 Pyrex bulb attached to a modified rotary evaporator (Laborota 4000 efficient, Heidolph) was used to study the heterogeneous photodegradation of molecular iodine adsorbed on solid SiO_2 particles in the presence of solar radiation in the ultraviolet and visible region of the solar spectrum [23]. Under typical experimental conditions, about 500 mg of dried SiO_2 particles coated with molecular iodine was placed within the Pyrex bulb. The bulb was attached to the modified rotary evaporator and immersed in a temperature-controlled bath. The Xenon Lamp 300W was used to irradiate the sample within the Pyrex bulb across its wall. The bulb was allowed to rotate to ensure that the I_2-coated particles within the Pyrex bulb were well homogenized, assuring that all the particles were well exposed to the incoming UV and visible radiation.

A continuous flow of synthetic air was allowed to enter the bulb volume. The synthetic air was generated using a benchtop zero air generator. Briefly, zero air generators produce laboratory grade purified air by completely removing hydrocarbons, CO_2, NOx (NOx = NO + NO_2) and H_20 from the air stream. This avoids the need to use inconvenient air cylinders, which may be dangerous for laboratory conditions.

The total air flow (250 sccm) was controlled using a mass flow controller and the bulb volume was renewed every two minutes. The experimental flow dynamics were limited by the rate of

desorption of molecular iodine adsorbed on the solid media and the gas-particle exchange. That is, the given gas flow rate was used in order to renew the bulb gaseous volume fast enough (to avoid a significant I_2 re-adsorption on the silica and to limit a gas-silica equilibrium) without accelerating the phisico-desortpion in an unreasonable manner (it would prevent us from obtaining a reliable estimation of the photodisssociation rate or *J*-value (see Equation 1). Part of the main flow was diverted using a restriction needle valve and allowed to enter two bubblers placed in a series and filled with ultra-pure water to obtain the desired humidity. The relative humidity was measured directly in the gas flow using a hygrometer "Hygrolog NT2" (Rotronic) with "HygroClip SC04" probe. The instrument accuracy of relative humidity measurements was ±1.5%.

Two sets of experiments were carried out. In the first set of experiments, the measured temperature within the Pyrex bulb was $T = (298\pm1)$K and the resulting relative humidity ranged from ≤ 2% to 75% RH under given experimental conditions. In the second set of experiments, the measured relative humidity within the Pyrex bulb was 40%RH and the temperature ranged from $283\pm1 \leq T(\mathrm{K}) \leq 323\pm1$, values representative of the typical lower atmosphere conditions.

$\underline{SiO_2 \text{ particles}}$

To simulate the complex physical and chemical nature of atmospheric aerosol content, AEROSIL R812 silica particles were used [23] to study the influence of the temperature and relative humidity on the heterogeneous photo-degradation of I_2. These model particles were chosen because it has been estimated that as much as 20 to 30% of the atmospheric particles' content includes SiO_2. The siloxane surface of the AEROSIL R812 silica particles is, therefore, a good first approximation of the inorganic oxide particle content found in the atmosphere and will assist the scientific community to advance the understanding of chemisorption and reactive fate of molecular iodine adsorbed on aerosols in the atmosphere. The AEROSIL R812

(Silanamine, 1,1,1-trimethyl-N-(trimethylsilyl)-, hydrolysis products with silica; CAS Number: 68909-20-6) was purchased from Evonic Degussa GmbH and the stated minimum SiO_2 content was ≥99.8%. AEROSIL R812 is a fumed silica aftertreated with organosilane with high specific surface and marked hydrophobia. The stated specific surface area (based on Brunauer-Emmett-Teller (BET) analysis conducted at the boiling temperature of N_2, 77K) was 260±30 m^2/g (AEROSIL, 2014, p. 812) and the stated average particle size was 7 nm. However, the SiO_2 particles are known to agglomerate to form an aerosol of a few micrometers in diameter, reflecting atmospheric-like suspended matter [33]. Particle density was 60 g/L.

Coating of SiO_2 particles

Molecular iodine was coated on the SiO_2 particles surface using a liquid/solid adsorption method as reported in our earlier work [23]. The particles coating was carried out in the absence of UV visible radiation to minimize any photo-degradation of molecular iodine. In a typical coating procedure, 500 mg of SiO_2 particles were placed within the 500 cm^3 Pyrex bulb and 100 mL of 9 mg/L I_2/cyclohexane (HPLC grade, ≥99.8%, Sigma-Aldrich) solution was added to the mix. The bulb with its contents was then placed in an ultrasonic bath for 15 minutes to homogenize the mixture. After, the liquid cyclohexane fraction of the mix was removed under aspirator vacuum (Rotavapor R-114, Büchi) at T = 313K and p = (25.6±2) MPa for 45 minutes. Assuming a uniform particle surface coverage for the iodine molecules and a spherical particle geometry, the percentage of the particle surface coated with iodine was estimated to be ~0.2% of the monolayer for hydrophobic silica [34].

Extraction and molecular iodine quantification

Similar to our previous work [23], the 2,4,6-tribromoaniline internal standard and the N,N-dimethylaniline derivatization reagent were used to quantify the molecular iodine adsorbed on solid SiO_2 particles. Under typical experimental conditions, 30 mg of the sample was extracted

from the Pyrex bulb every 30 minutes and placed in an air-tight vial. After, 50 μL of the internal standard and 50 μL of the 300 mg/L N,N-dimethylaniline/cyclohexane solution was added to the vial. The vial was then hermetically sealed and stored at T=-20°C until the following day. Subsequently, contents of the vial were placed in a stainless-steel compartment volume of the Accelerated Solvent Extraction (ASE 300, Dionex) system and topped-off with 33 mL of cyclohexane solvent. Three ASE cycles were performed. The first 5-minute cycle of the ASE extraction process was allowed to take place at T = 100°C and p = 100 bar. After, 50% (~16.5 mL) of the ASE cell volume was automatically extracted and then resulting aliquot was placed in a separate ASE stainless-steel compartment volume. The original ASE cell was then topped-off with cyclohexane to 33 mL total volume. The extraction process was then repeated two more times. After the final, third, cycle, the total volume of the ASE cell was retrieved (33 mL). The net final volume (~70 mL) was then enriched under a steady flow of nitrogen gas using the TurboVapII (Biotage) workstation. The nitrogen gas flow temperature was kept at T = 50°C and the N_2-gas head pressure was p = 5 bar. The obtained extract solution was concentrated down to a final volume of 500 μL. The obtained 500 μL extract was then filtered using a PTFE (0.22 μm pore size) membrane filter and analyzed using the TRACE GC Ultra gas chromatography (Thermo Scientific) and quantified using the TSQ Quantum Triple Quadrupole Mass Spectrometer (Thermo Scientific). A Thermo TG-5MS capillary column (30 m × 0.25 mm i.d., 0.25 μm) was used. The helium (99.999%, Air Liquide) carrier gas flow rate was 1 mL/min. Liquid samples were injected in the split mode (1:50) and the injector temperature was maintained at T = 220°C. The initial GC oven temperature was held at T = 35°C for one minute and then the oven temperature was stepped-up at the rate of 30 °C/min to 220°C and then held at T = 220°C for 11 minutes. The transfer line temperature between the GC and the MS/MS analyzer was T = 280°C. The MS/MS analyzer was operated in a full scan/single ion monitoring

mode to increase the sensitivity and the MS/MS system electron impact ionization energy was 70 eV.

Photolytic light source

Similar to our previous work [23], the 300 W high pressure Xenon lamp (LOT, Oriel) was used as the solar radiation source to irradiate the I_2-SiO_2 mixture located within the Pyrex reactor. The Xenon lamp solar radiation spectrum and the discussion concerning the radiometric measurements within the Pyrex reactor are published elsewhere [23].

Results and discussion

Rate of photolysis of I_2

Similar to our previous work [23], the kinetics of the heterogeneous photolysis of I_2 on SiO_2 particles were determined by monitoring the loss of I_2 as a function of time. The photolytic loss of molecular iodine adsorbed on SiO_2 particles exhibited an exponential decay, implying first-order kinetics (Equation 1).

$$\frac{d[I_2]}{dt} = -k_{obs}[I_2] = -(k_{desorption} + J)[I_2] \quad (1)$$

In Equation. 1, $k_{obs}(s^{-1})$ is the observed first-order rate constant, $k_{desorption}(s^{-1})$ is the desorption first-order rate constant, $J(s^{-1})$ is the photodissociation rate constant, t(s) is the time of exposure to solar radiation and $[I_2]$ is the normalized iodine concentration adsorbed on the silica particles.

"Dark" desorption and hydrolysis of iodine adsorbed on SiO_2 particles

Since the vapor pressure of solid molecular iodine is about $33.3 \leq p(Pa) \leq 41.3$ [35–37] at T = 20°C, part of the initial amount of I_2 adsorbed on SiO_2 particles will certainly volatilize over time. To account for this loss of iodine due to desorption and/or hydrolysis ($k_{desorption}$), background control experiments were carried out in the absence of photolytic radiation under

given experimental conditions of temperature and relative humidity. As shown in an earlier study, heterogeneous reactivity of pendimethalin adsorbed on AEROSIL R812 particles was observed to decrease with increasing relative humidity [38]. To account for this "hydrophobic" effect, experiments were carried out at T = 298K and relative humidity (RH) values ranging from ≤ 2% to 75%RH. Values of first-order kinetic constants $k_{desorption}$ at different humidity values are presented in the Table 1 and shown in Figure 1. As presented in Table 1 and illustrated in Figure 1, the first-order rate constant $k_{desorption}$ accounts for the background desorption of I_2 from the SiO_2 surface, hydrolysis of I_2 due to a presence of water on SiO_2 surfaces and other losses. As shown in Figure 1, no clear dependence of $k_{desorption}$ on relative humidity is observed. Two reproducibility experiment were performed at 0% and 20%RH and led to a desorption kinetics values well within the uncertainty bars shown in Figure 1. As a result, iodine loss observed in our experimental conditions are expected to be due to desorption rather than hydrolysis; hydrolysis is expected to occur for higher RH values than those studied in this work.

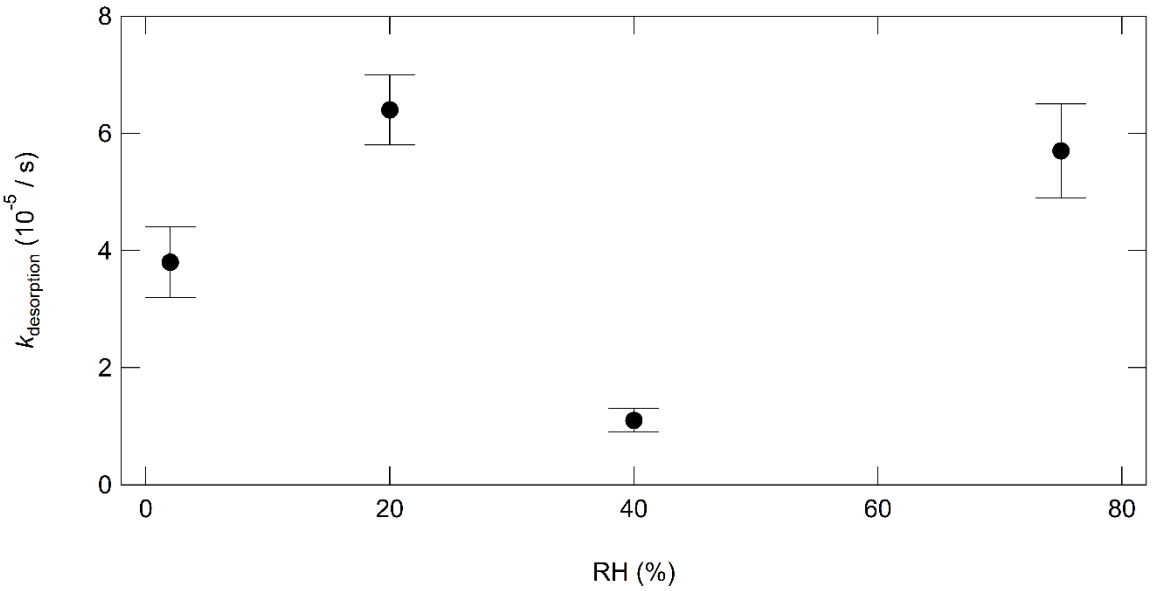


Figure 1 Plot of the obtained first-order rate constants ($k_{desorption}$) for the desorption of iodine as a function of relative humidity. No clear dependence of humidity on the desorption rate constant of I_2 adsorbed on SiO_2 particles is observed. The quoted uncertainties in $k_{desorption}$, values are 68% (1σ) confidence limits from the linear regression fit.

214 Influence of humidity on the photo-degradation of I_2 on SiO_2 particles (k_{obs})

215 It is known that water in all its phases plays an important role in global warming and
216 atmospheric chemistry. Water is a known green-house gas, albeit all-important and
217 indispensable for life on Earth, and an atmospheric precursor of hydroxyl radicals responsible
218 for the oxidative capacity of the atmosphere. Further, it is known that mono- and multi-layer
219 water films form on atmospheric particles when the relative humidity is 30% or greater [26].
220 This is important since the kinetics of many heterogeneous, surface or interface reactions
221 depend on the type of aerosol particle phase and surface morphology and physico-chemical
222 properties and behavior [27]. As a result, the influence of humidity on the photo-oxidation of
223 I_2 on SiO_2 particles (k_{obs}) is studies.

224 Typical normalized iodine concentration temporal profiles for experiments carried out at T =
225 298K and ≤ 2 to 75%RH in the absence ("dark" conditions) and presence of simulated solar
226 radiation are shown in shown in Figure 2 and Figure 3, respectively. The obtained $k_{desorption}$ and
227 k_{obs} rate constants are listed in Table 1.

228 *Table 1. Summary of kinetic data for the photolysis of I_2 adsorbed on SiO_2 particles carried out*
229 *at T = 298K and (2 - 75)%RH in a Pyrex reactor and using 300W Xe lamp photolysis. The*
230 *listed errors in %RH are estimated systematic errors associated with measuring the relative*
231 *humidity. The quoted uncertainties in the $k_{desorption}$, $k_{observed}$ and J values are 68% (1σ)*
232 *confidence limits from the linear regression fit. [1]: Dark condition. [2]: Xe lamp photolysis*

%RH	$k_{desorption}$ [1] (10^{-5}/s)	$k_{observed}$ [2] (10^{-5}/s)	J (10^{-5}/s)	τ (min)
2±2	3.8±0.6	11.1±1.1	7.3±1.2	228
20±2	6.4±0.6	13.4±1.6	7.0±1.0	238
40±2[§]	1.1±0.2	10.0±1.1	8.9±1.1	187
75±2	5.7±0.8	14.9±1.6	9.2±1.1	160

233 [§] [23]

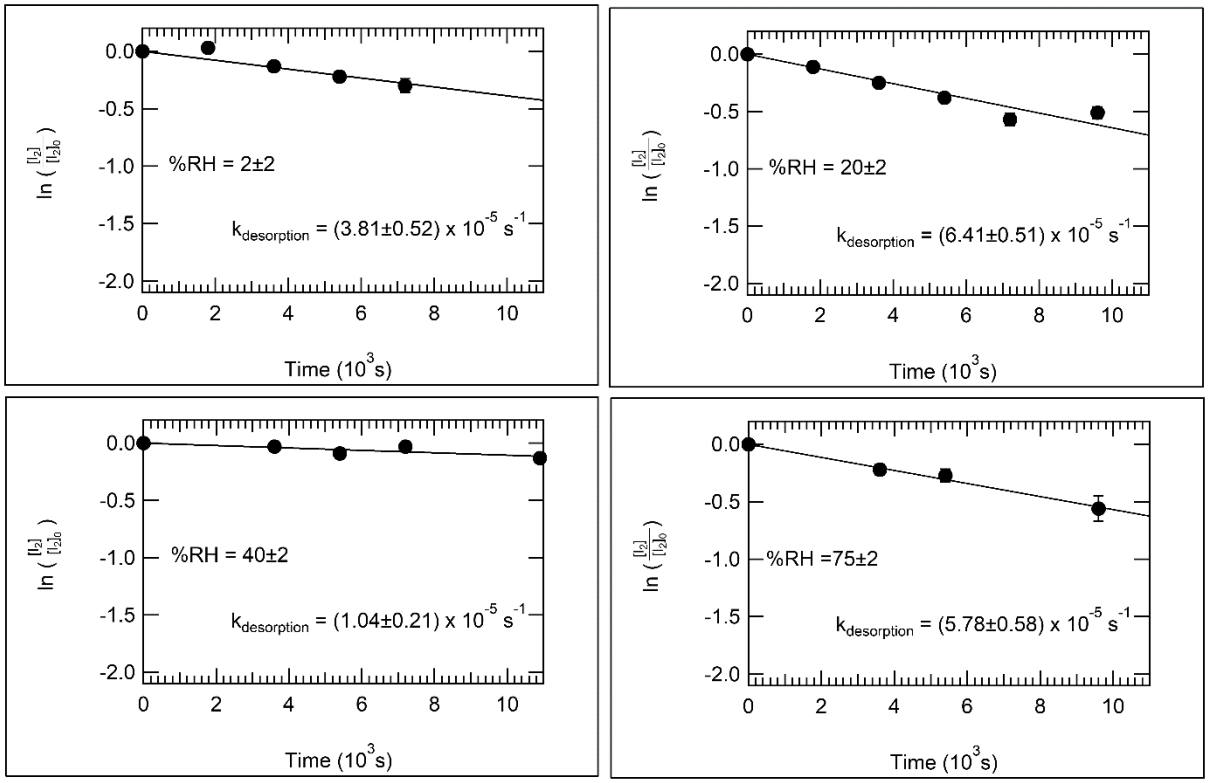


Figure 2. Typical normalized iodine concentration temporal profiles for experiments carried out at T = 298K and ≤ 2 to 75 %RH in the absence of simulated solar radiation ("dark" conditions). The solid lines are obtained from least squares analyses and give the expressions for $k_{desorption}$ shown in the figure. The error bars in %RH are estimated systematic errors

associated with measuring the relative humidity. The quoted uncertainties in k_{obs} are 68% (1σ) confidence limits from the linear regression fit.

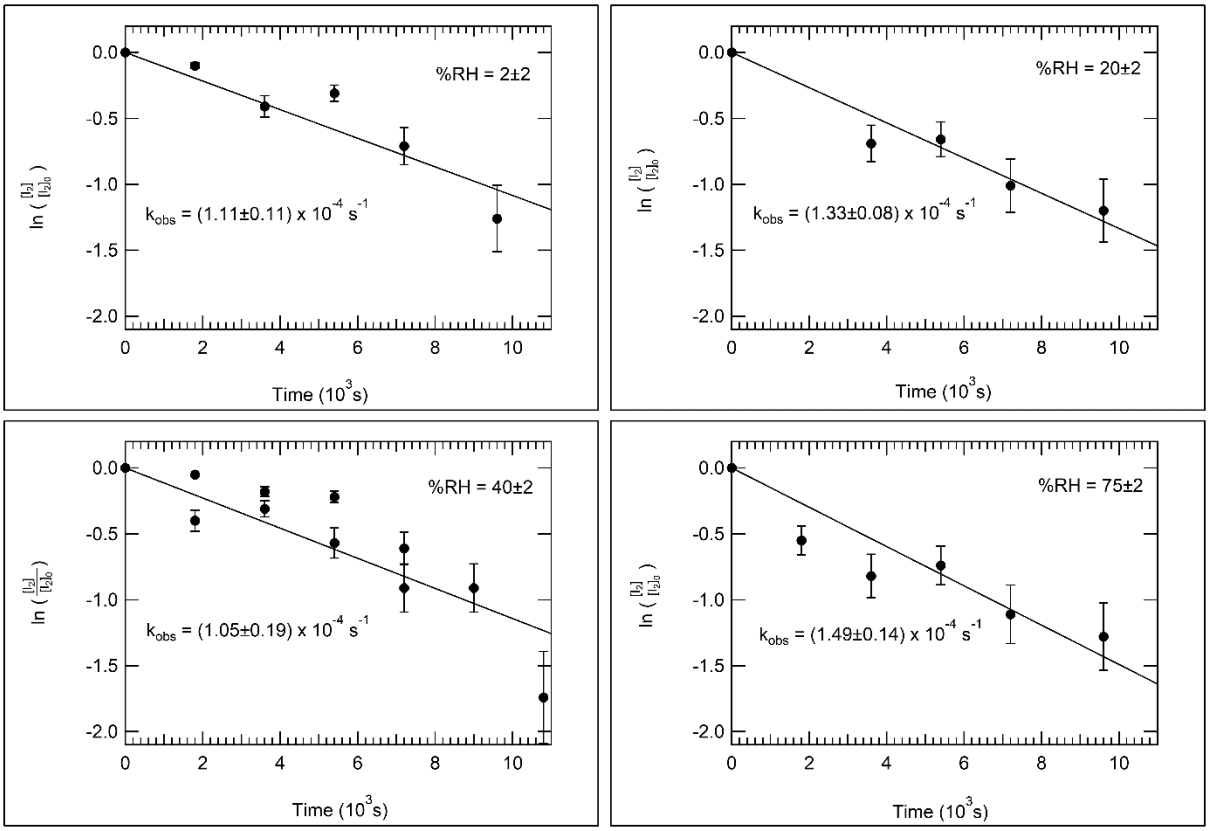


Figure 3. Typical normalized iodine concentration temporal profiles for experiments carried out at T = 298K and (2 - 75)%RH following photolysis of the I_2 adsorbed on SiO_2 particles. The solid lines are obtained from least squares analyses and give the expressions for k_{obs} shown in the figure. The error bars in %RH are estimated systematic errors associated with measuring the relative humidity. The quoted uncertainties in k_{obs} are 68% (1σ) confidence limits from the linear regression fit.

As listed in Table 1, the photodissociation rate constant, *J*, for I_2 adsorbed on SiO_2 particles, is obtained from the difference in the desorption rate constant, $k_{\text{desorption}}$, and the observed photolysis rate constant, k_{obs} (see Equation 1). The $k_{\text{desorption}}$ accounts for 10% to 50% of the observed k_{obs} which is small enough to quantify in a relevant manner the photodissociation rate constant, *J*-value, and confirms that the given experimental gas flow rate within the bulb is appropriate for these experiments. Plot of the obtained first-order rate constants for the heterogeneous photolysis of iodine as a function of relative humidity is shown in Figure 4. As

shown in Figure 4, no clear dependence of the photodissociation rate constant on relative humidity is observed. As a result, the average photodissociation rate constant is calculated to give $J = (8.2 \pm 1.1) \times 10^{-5}/\mathrm{s}$ at *T*=298K independent of relative humidity under the experimental conditions employed. Based on the obtained *J*-value, the photolytic lifetime of I_2 adsorbed on SiO_2 particles is calculated to be approximately 203 minutes or 3.4 hours.

The absence of the dependence on humidity of the photodissociation rate constant of I_2 adsorbed on SiO_2 particles may be explained by its low solubility (300 mg/L) in water [36,39]. Further, the observed non-dependence may also be explained by the type of SiO2 particles used in this work, that is, hydrophobic AEROSIL R812 silica particles. These particles are known to prevent water film formation on their surfaces. However, these "hydrophobic" effect on AEROSIL R812 silica particles may decrease with increasing gas-phase water content. Further, these types of "hydrophobic" particles are often used by atmospheric scientists to study real-life atmospheric behavior of aerosols. At higher humidity levels, the water surface coverage of AEROSIL R812 silica particles is known to approach real-life atmospheric particle physiology. Nonetheless, to confirm the obtained results in this work, other types of particles with different surface physico-chemical characteristics that better represent the complex nature of atmospheric aerosols need to be studied.

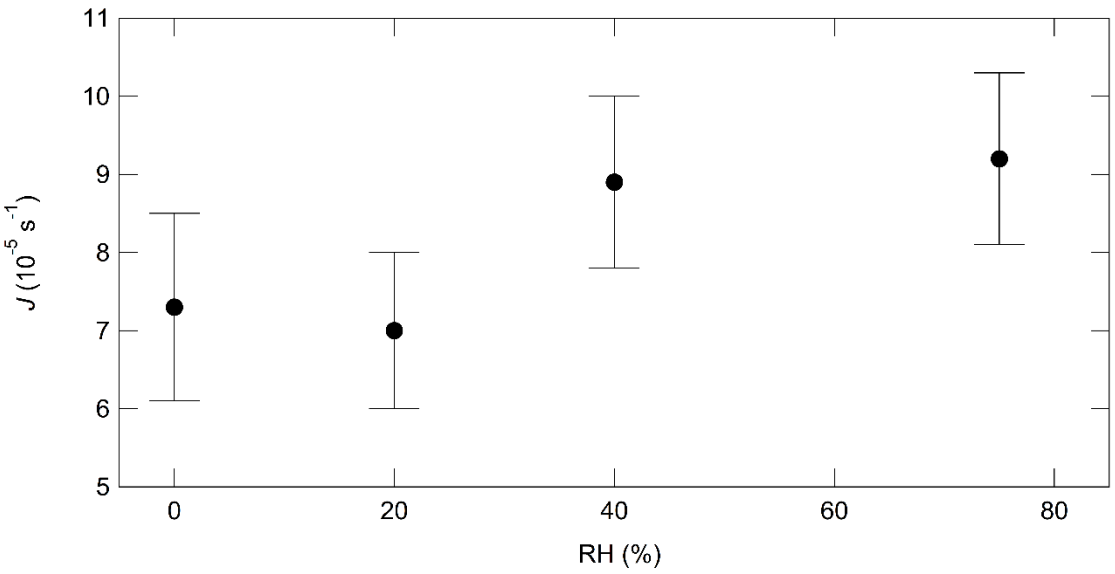


Figure 4. Plot of the obtained first-order rate constants for the heterogeneous photolysis of iodine as a function of relative humidity. No clear influence of humidity on the photodissociation rate constant of I_2 adsorbed on SiO_2 particles is observed.

Influence of the temperature on the photo-degradation of I_2 on SiO_2 particles

To better understand the real atmosphere behavior and fate of molecular iodine adsorbed on solid particles, a set of heterogeneous photolysis experiments was performed at different temperatures that reflect more realistic environment conditions [40]. Typical normalized iodine concentration temporal profiles for experiments carried out at 40%RH and $283 \leq T(K) \leq 323$ temperature range under "dark" conditions and following the photolysis of the I_2/SiO_2 solid are shown in Figure 5 and Figure 6, respectively. As shown in Figure 5, the $k(T)_{desorption}$ values are obtained from experiments carried out under "dark" conditions, that is, in the absence of solar radiation. In a similar manner, as shown in Figure 6, the $k(T)_{obs}$ values are obtained from experiments in the presence of simulated solar radiation. The obtained $k(T)_{desorption}$ and $k(T)_{obs}$ rate constants are listed in Table 2.

Table 2 Summary of kinetic data for the photolysis of I_2 adsorbed on SiO_2 particles carried out at the $283 \leq T(K) \leq 323$ temperature range and at 40%RH in a Pyrex reactor and using 300W Xe lamp photolysis. The listed errors in temperature are estimated systematic errors associated

with the measurement. The quoted uncertainties in the $k_{desorption}$, $k_{observed}$ and J values are 68% (1σ) confidence limits from the linear regression fit. [1]: Dark condition. [2]: Xe lamp photolysis

T (K)	$k_{desorption}$ [1] (10^{-5}/s)	$k_{observed}$ [2] (10^{-5}/s)	J (10^{-5}/s)	τ [&] (min)
283±2	8.1±0.6	14.7±1.1	6.6±1.3	252
298±2 [§]	1.1±0.1	10±1.1	8.9±1.1	187
308±2	12.1±1.1	22.2±1.4	10.1±1.1	165
315±2	4.6±1.2	14.1±1.1	9.5±1.6	175
323±2	5.7±0.8	19.8±1.8	14.1±1.8	119

[§] [23]

[&] The atmospheric residence time $\tau = \mathbf{1}/J(T)$

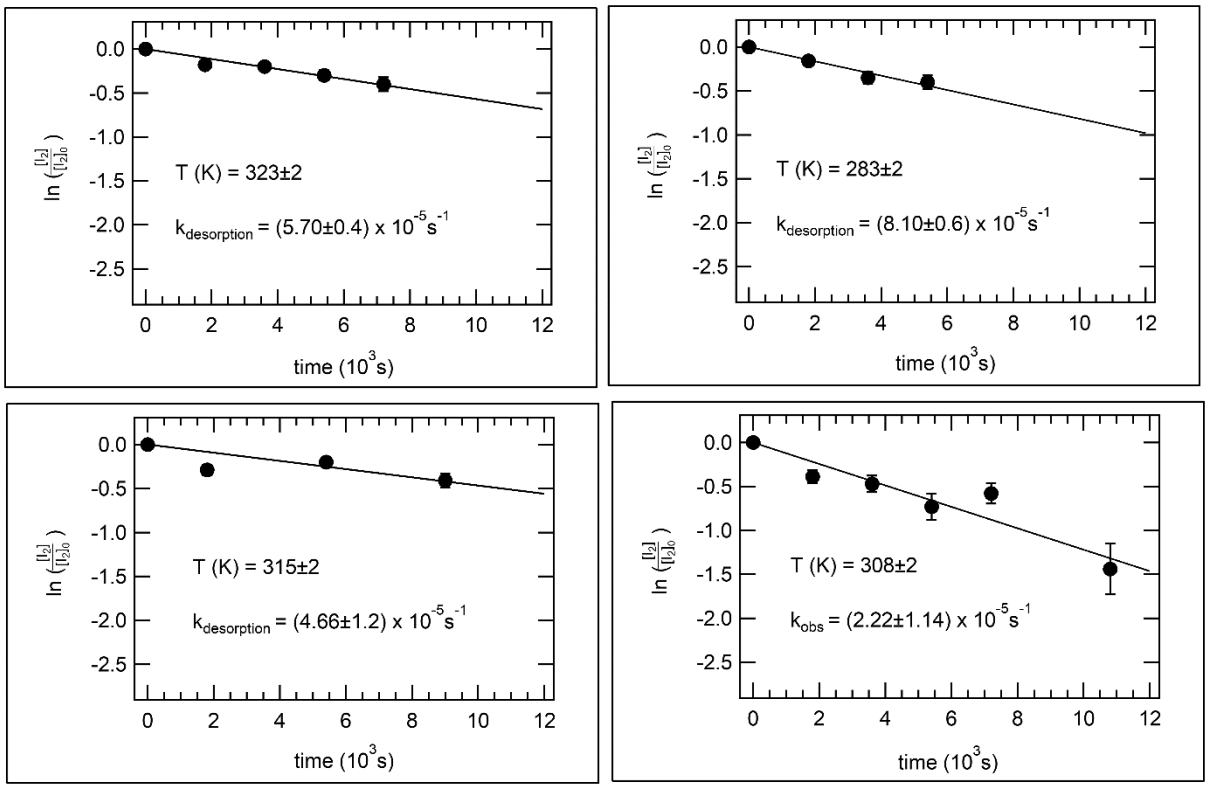


Figure 5. Typical normalized iodine concentration temporal profiles for experiments carried out in the 283 ≤ T(K) ≤ 323 temperature range and at 40%RH in the absence of photolysis ("dark" conditions) of the I_2 adsorbed on SiO_2 particles.

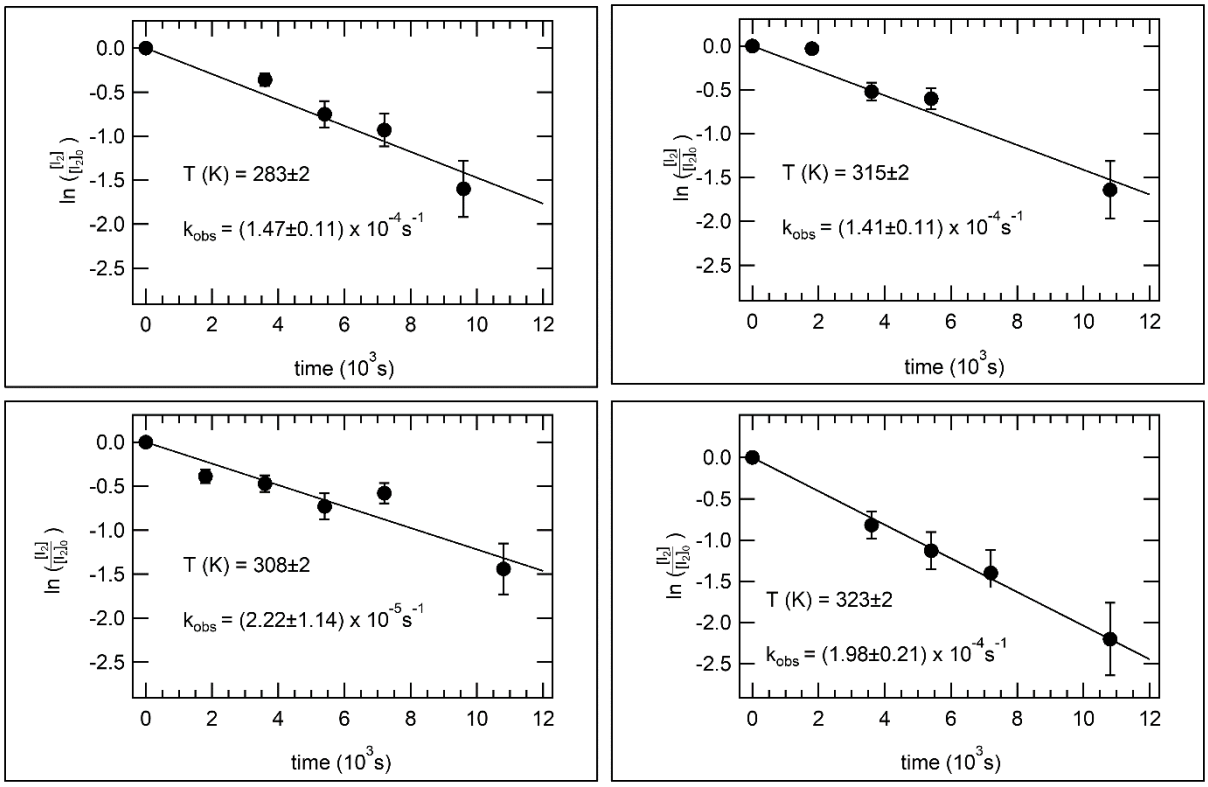
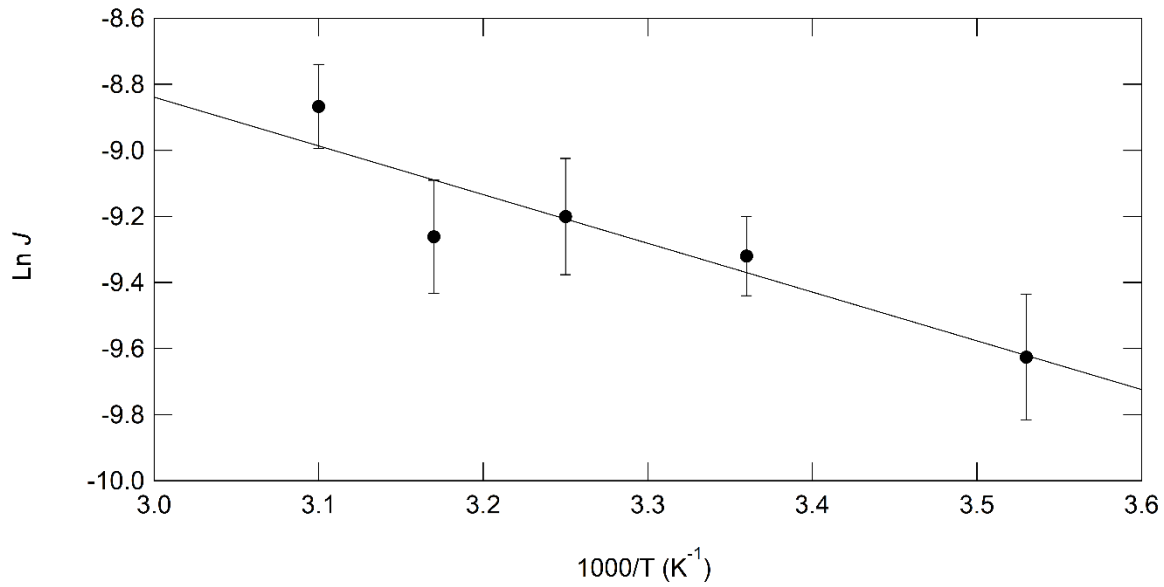


Figure 6 Typical normalized iodine concentration temporal profiles for experiments carried out in the 283 ≤ T(K) ≤ 323 temperature range and at 40%RH following photolysis of the I_2 adsorbed on SiO_2 particles. The solid lines are obtained from least squares analyses and give the expressions for k_{obs} shown in the figure. The quoted uncertainties in the $k_{observed}$ values are 68% (1σ) confidence limits from the linear regression fit.

Similar to the situation listed above, the photodissociation rate constant, *J(T)*, for I_2 adsorbed on SiO_2 particles, is calculated from the difference in the experimentally obtained desorption rate constant, $k_{desorption}$, and the experimentally obtained rate constant, k_{obs}. The photodissociation rate constant (*J*-value) for the photo-degradation of I_2 on solid SiO_2 particles does not appear to be humidity dependent under the experimental conditions employed (< 55% of the total contribution). On the other hand, the *J*-value for the photo-degradation of I_2 on solid SiO_2 particles is observed to be temperature dependent in the temperature range T = 283K to T = 323K. Plot of the obtained natural logarithm of the obtained *J*(K) value for the heterogeneous photolysis of molecular iodine as a function of temperature is shown in Figure 7. As shown in Figure 7, a clear dependence of the photodissociation rate constant on temperature is observed.



316

317 *Figure 7 Arrhenius plot for photolysis of the I_2 adsorbed on SiO_2 particles. The solid line is*
318 *obtained from a least-squares analysis and given the following Arrhenius expression:*
319 $J\ (T) = (1.24 \pm 1.4) \times 10^{-2} \times exp[(1482 \pm 345)/T]\ /s$. *The uncertainties in the expression*
320 *are* 1σ *and represent precision only.*

321 The following Arrhenius expression is derived from the data:

322 $$\mathrm{J\ (T)} = (1.24 \pm 1.4) \times 10^{-2} \times \exp[(1482 \pm 345)/\mathrm{T}]\ \mathrm{s^{-1}}$$

323 Uncertainties in the above expression are ±1σ and represent precision only and refer to the
324 Arrhenius parameters only. The activation energy for the photodissociation reaction of I_2 on
325 SiO_2 particles is rounded-off to be 12.3±2.9 kJ/mol.

326 As stated above, the *J(T)* value is calculated from the difference in the experimentally obtained
327 desorption rate constant, $k_{\mathrm{desorption}}$, and the experimentally obtained rate constant, k_{obs}. As listed
328 in Table 1 and Table 2 and shown in the Figure 8 below, there is no clear humidity dependence
329 on the obtained $k_{\mathrm{desorption}}$ and k_{obs} values. However, such an influence on humidity of the
330 obtained *k*-values cannot be excluded.

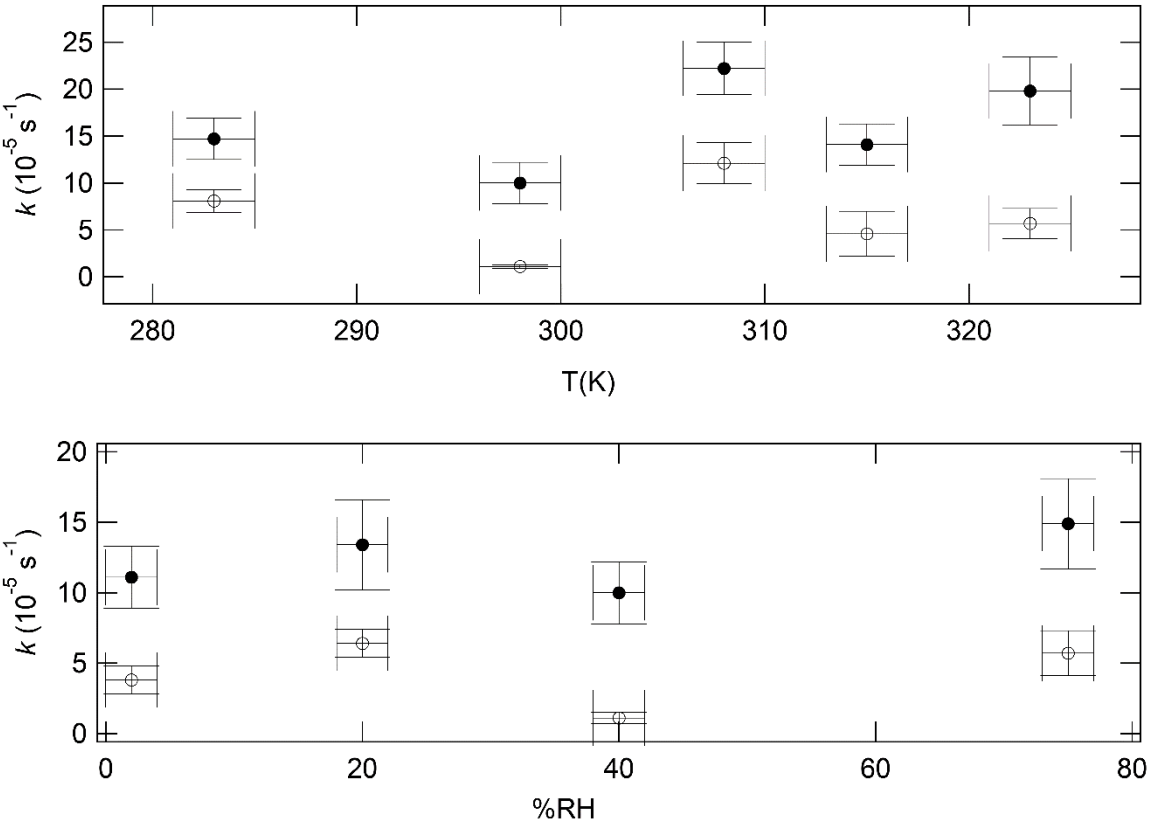


Figure 8. Comparison of the experimentally obtained desorption rate constant, $k_{desorption}$, (○ open circles) and the experimentally obtained rate constant, k_{obs} values (● closed circles) as a function of temperature (above) and relative humidity (below). The uncertainties in the k values are 95% (2σ) confidence limits. The uncertainties in the temperature are ±2K, experimental estimation.

On the other hand, as shown in Figure 8, while there does not appear to be a clear temperature dependence on the $k_{desorption}$ values, the obtained k_{obs} rate constants do appear to be temperature dependent. The observed discrepancies may be explained by the physico-chemical surface properties of the AEROSIL R812 particles used in this work. That is, the AEROSIL R812 surfaces are coated with organo-silane compounds and treated at T=105°C for 2 hours before being commercialized. The AEROSIL surfaces are thus assumed to be chemically inert and "stable" under the experimental conditions (283K-323K) employed in this work. Nevertheless, chemical rearrangements on the AEROSIL R812 surfaces cannot be fully excluded that may have induced the observed influence of the $k_{desorption}$ (dark conditions) on the experimental the

%RH and temperature. As a result, the physico-chemical interactions of I_2 on silica surfaces may differ at given experimental RH and temperature conditions. However, the observed influence of the temperature seems to have only a minor effect on the estimation of the photolysis rate constant as shown in Figure 7.

Conclusion

The heterogeneous photodegradation of I_2 on solid surfaces was studied at T(K) = 283 to T(K) = 323K and from ≤ 2%RH to ≤ 75%RH in synthetic air to better understand its atmospheric fate. The results reported in this work demonstrate that the calculated J-value is observed to be temperature dependent over the temperature range studied. This photolysis rate constant may be expressed by $J(\mathrm{T}) = (1.24 \pm 1.4) \times 10^{-2} \times \exp[(1482 \pm 345)/\mathrm{T}]\ /s$ over the measured temperature range. The heterogeneous atmospheric residence time ($\tau = 1/J(\mathrm{T})$) of I_2 adsorbed on solid media is calculated to range from 2 to 4.1 hours.

This work complements and completes the previous study on the photodegradation of molecular iodine adsorbed on model SiO_2 particles [23]. The obtained results will help to improve the calculation of the evolution of molecular iodine dispersion and transport in the atmosphere. More generally, the obtained results will help the industrial and academic communities to better understand and predict the environmental fate of I_2 adsorbed on the particle surfaces. However, to better understand and model real-atmosphere heterogeneous behavior of I_2, other studies need to be included that include other particle surfaces with different physico-chemical properties to better understand and model the atmospheric dispersion and environmental fate of I_2.

Acknowledgements

We gratefully acknowledge financial support in a form of a doctoral grant from the *Institut de Radioprotection et de Sûreté Nucléaire* (IRSN) and the *Region Sud.*

Nomenclature

CCN	=	cloud condensation nuclei
eV	=	electron volt
HPLC	=	High Performance Liquid Chromatography
$J(T)$	=	photolysis rate constant (1/s) as a function of temperature, T.
KIE	=	Kinetic Isotope Effect
$k_{desorption}$	=	desorption first-order-rate constant (1/s)
k_{obs}	=	observed first-order-rate constant (1/s)
mg	=	milligram
μL	=	microliter
mL	=	milliliter
MS	=	mass spectrometry
MS/MS	=	tandem mass spectrometry
%RH	=	percent relative humidity
pptv	=	parts per trillion per volume
σ	=	standard deviation
t	=	time (s)
W	=	Watt

References

[1] Buseck, P. R., and Pósfai, M., 1999, "Airborne Minerals and Related Aerosol Particles: Effects on Climate and the Environment," *Proc. Natl. Acad. Sci.*, 96(7), pp. 3372–3379.

[2] Baker, A. R., Thompson, D., Campos, M. L. A. M., Parry, S. J., and Jickells, T. D., 2000, "Iodine Concentration and Availability in Atmospheric Aerosol," *Atmos. Environ.*, 34(25), pp. 4331–4336.

[3] Garland, J. A., and Curtis, H., 1981, "Emission of Iodine from the Sea Surface in the Presence of Ozone," *J. Geophys. Res. Oceans*, 86(C4), pp. 3183–3186.

[4] Saiz-Lopez, A., Plane, J. M. C., Baker, A. R., Carpenter, L. J., Von Glasow, R., G Omez Martín, J. C., Mcfiggans, G., and Saunders, R. W., 2012, "Atmospheric Chemistry of Iodine," *Chem Rev*, 112, pp. 1773–1804.

[5] Bitter, M., Ball, S. M., Povey, I. M., and Jones, R. L., 2005, "A Broadband Cavity Ringdown Spectrometer for In-Situ Measurements of Atmospheric Trace Gases," *Atmospheric Chem. Phys.*, 5(9), pp. 2547–2560.

[6] Finley, B. D., and Saltzman, E. S., 2008, "Observations of Cl2, Br2, and I2 in Coastal Marine Air," *J. Geophys. Res. Atmospheres*, 113(D21).

[7] Huang, R.-J., Seitz, K., Buxmann, J., Pöhler, D., Hornsby, K. E., Carpenter, L. J., Platt, U., and Hoffmann, T., 2010, "In Situ Measurements of Molecular Iodine in the Marine Boundary Layer: The Link to Macroalgae and the Implications for O 3, IO, OIO and NO x," *Atmospheric Chem. Phys.*, 10(10), pp. 4823–4833.

[8] Leigh, R. J., Ball, S. M., Whitehead, J., Leblanc, C., Shillings, A. J. L., Mahajan, A. S., Oetjen, H., Lee, J. D., Jones, C. E., and Dorsey, J. R., 2010, "Measurements and Modelling of Molecular Iodine Emissions, Transport and Photodestruction in the Coastal Region around Roscoff," *Atmospheric Chem. Phys.*, 10(23), pp. 11823–11838.

[9] Mahajan, A. S., Oetjen, H., Saiz-Lopez, A., Lee, J. D., McFiggans, G. B., and Plane, J. M., 2009, "Reactive Iodine Species in a Semi-polluted Environment," *Geophys. Res. Lett.*, 36(16).

[10] Mahajan, A. S., Plane, J. M. C., Oetjen, H., Mendes, L., Saunders, R. W., Saiz-Lopez, A., Jones, C. E., Carpenter, L. J., and McFiggans, G. B., 2010, "Measurement and Modelling of Tropospheric Reactive Halogen Species over the Tropical Atlantic Ocean," *Atmospheric Chem. Phys.*, 10(10), pp. 4611–4624.

[11] Peters, C., Pechtl, S., Stutz, J., Hebestreit, K., Hönninger, G., Heumann, K., Schwarz, A., Winterlik, J., and Platt, U., 2005, "Reactive and Organic Halogen Species in Three Different European Coastal Environments," *Atmospheric Chem. Phys.*, 5(12), pp. 3357–3375.

[12] Saiz-Lopez, A., Saunders, R. W., Joseph, D. M., Ashworth, S. H., and Plane, J. M. C., 2004, *Atmospheric Chem. Phys. Discussions*, 4, pp. 2379-2403.

[13] Saiz-Lopez, A. J. M. C. P., Plane, J. M. C., McFiggans, G., Williams, P. I., Ball, S. M., Bitter, M., Jones, R. L., Hongwei, C., and Hoffmann, T., 2006, "Modelling Molecular Iodine Emissions in a Coastal Marine Environment: The Link to New Particle Formation," *Atmospheric Chem. Phys.*, 6(4), pp. 883–895.

[14] Kinoshita, N., Sueki, K., Sasa, K., Kitagawa, J., Ikarashi, S., Nishimura, T., Wong, Y.-S., Satou, Y., Handa, K., Takahashi, T., and others, 2011, "Assessment of Individual Radionuclide Distributions from the Fukushima Nuclear Accident Covering Central-East Japan," *Proc. Natl. Acad. Sci.*, 108(49), pp. 19526–19529.

[15] Momoshima, N., Sugihara, S., Ichikawa, R., and Yokoyama, H., 2012, "Atmospheric Radionuclides Transported to Fukuoka, Japan Remote from the Fukushima Dai-Ichi

Nuclear Power Complex Following the Nuclear Accident," *J. Environ. Radioact.*, 111, pp. 28–32.
[16] Loewenstein, L. M., and Anderson, J. G., 1985, "Rate and Product Measurements for the Reactions of Hydroxyl with Molecular Iodine and Iodine Chloride at 298 K: Separation of Gas-Phase and Surface Reaction Components," *J. Phys. Chem.*, 89(25), pp. 5371–5379.
[17] Koutsenogii, P. K., and Jaenicke, R., 1994, "Number Concentration and Size Distribution of Atmospheric Aerosol in Siberia," *J. Aerosol Sci.*, 25(2), pp. 377–383.
[18] Sharma, D., Rai, J., Israil, M., and Singh, P., 2003, "Summer Variations of the Atmospheric Aerosol Number Concentration over Roorkee, India," *J. Atmospheric Sol.-Terr. Phys.*, 65(9), pp. 1007–1019.
[19] Chamberlain, A. C., 1960, "Aspects of the Deposition of Radioactive and Other Gases and Particles," *Intern J Air Pollut.*, 3.
[20] Chamberlain, A. C., and Chadwick, R. C., 1966, "Transport of Iodine from Atmosphere to Ground," *Tellus*, 18(2–3), pp. 226–237.
[21] Gard, E. E., 1998, "Direct Observation of Heterogeneous Chemistry in the Atmosphere," *Science*, 279(5354), pp. 1184–1187.
[22] Shen, X., Zhao, Y., Chen, Z., and Huang, D., 2013, "Heterogeneous Reactions of Volatile Organic Compounds in the Atmosphere," *Atmos. Environ.*, 68, pp. 297–314.
[23] Figueiredo, A., Strekowski, R. S., Bosland, L., Durand, A., and Wortham, H., 2020, "Photolytic Degradation of Molecular Iodine Adsorbed on Model SiO2 Particles," *Sci. Total Environ.*, p. 137951.
[24] Garland, J. A., 1967, "The Adsorption of Iodine by Atmospheric Particles," *J. Nucl. Energy*, 21(9), pp. 687–700.
[25] Megaw, W. J., 1965, "The Adsorption of Iodine on Atmospheric Particles," *J. Nucl. Energy. Parts A/B. React. Sci. Technol.*, 19(8), pp. 585–592.
[26] Keskinen, H., Romakkaniemi, S., Jaatinen, A., Miettinen, P., Saukko, E., Jorma, J., Mäkelä, J. M., Virtanen, A., Smith, J. N., and Laaksonen, A., 2011, "On-Line Characterization of Morphology and Water Adsorption on Fumed Silica Nanoparticles," *Aerosol Sci. Technol.*, 45(12), pp. 1441–1447.
[27] Knipping, E. M., 2000, "Experiments and Simulations of Ion-Enhanced Interfacial Chemistry on Aqueous NaCl Aerosols," *Science*, 288(5464), pp. 301–306.
[28] Coenen, H. H., Mertens, J., and Mazieère, B., 2006, Radiation Reactions For Pharmaceuticals. Compedium for Effective Synthesis Strategies, Springer Netherlands.
[29] Deitz, V. R., 1987, "Interaction of Radioactive Iodine Gaseous Species with Nuclear-Grade Activated Carbons," *Carbon*, 25(1), pp. 31–38.
[30] Rudolph, J., Czuba, E., and Huang, L., 2000, "The Stable Carbon Isotope Fractionation for Reactions of Selected Hydrocarbons with OH-Radicals and Its Relevance for Atmospheric Chemistry," *J. Geophys. Res. Atmospheres*, 105(D24), pp. 29329–29346.
[31] Rudolph, J., Czuba, E., Norman, A. L., Huang, L., and Ernst, D., 2002, "Stable Carbon Isotope Composition of Nonmethane Hydrocarbons in Emissions from Transportation Related Sources and Atmospheric Observations in an Urban Atmosphere," *Atmos. Environ.*, 36(7), pp. 1173–1181.
[32] Cantrell, C. A., Shetter, R. E., McDaniel, A. H., Calvert, J. G., Davidson, J. A., Lowe, D. C., Tyler, S. C., Cicerone, R. J., and Greenberg, J. P., 1990, "Carbon Kinetic Isotope Effect in the Oxidation of Methane by the Hydroxyl Radical," *J. Geophys. Res. Atmospheres*, 95(D13), pp. 22455–22462.
[33] Mattei, C., 2019, "Réactivité hétérogène de pesticides adsorbes sur des particules atmosphériques : Influence des paramètres environnementaux sur les cinétiques," *Ph.D. Thesis*, Aix-Marseille Université.

[34] Socorro, J., Gligorovski, S., Wortham, H., and Quivet, E., 2015, "Heterogeneous Reactions of Ozone with Commonly Used Pesticides Adsorbed on Silica Particles," *Atmos. Environ.*, 100, pp. 66–73.
[35] Baxter, G. P., Hickey, C. H., and Holmes, W. C., 1907, "The Vapor Pressure of Iodine," *J. Am. Chem. Soc.*, 29(2), pp. 127–136.
[36] Linstrom, P. J., and Mallard, W. G., 2020, "NIST Chemistry WebBook, NIST Standard Reference Database Number 69". Available at: https://doi.org/10.18434/T4D303.
[37] Stull, D. R., 1947, "Vapor Pressure of Pure Substances. Organic and Inorganic Compounds," *Ind. Eng. Chem.*, 39(4), pp. 517–540.
[38] Mattei, C., Wortham, H., and Quivet, E., 2019, "Heterogeneous Degradation of Pesticides by OH Radicals in the Atmosphere: Influence of Humidity and Particle Type on the Kinetics," *Sci. Total Environ.*, 664, pp. 1084–1094.
[39] Hartley, H., and Campbell, N. P., 1908, "LXIX.—The Solubility of Iodine in Water," *J Chem Soc Trans*, 93(0), pp. 741–745.
[40] Sander, S. P., 1986, "Kinetics and Mechanism of the Iodine Monoxide + Iodine Monoxide Reaction," *J. Phys. Chem.*, 90(10), pp. 2194–2199.